JACS
JOURNAL OF THE AMERICAN CHEMICAL SOCIETY

Subscriber access provided by ISTANBUL TEKNIK UNIV

Article

Effect of Confinement in Carbon Nanotubes on the Activity of Fischer#Tropsch Iron Catalyst

Wei Chen, Zhongli Fan, Xiulian Pan, and Xinhe Bao

J. Am. Chem. Soc., **2008**, 130 (29), 9414-9419 • DOI: 10.1021/ja8008192 • Publication Date (Web): 25 June 2008

Downloaded from http://pubs.acs.org on February 8, 2009

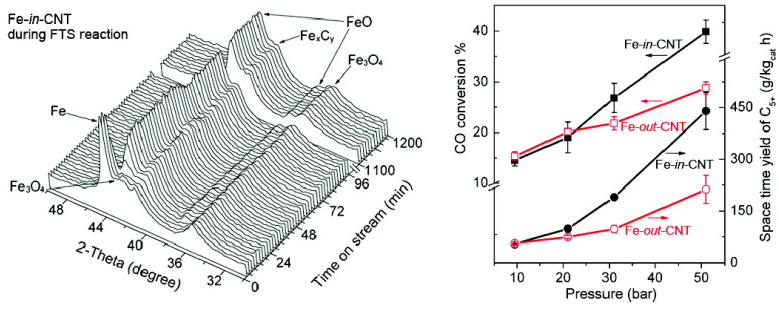

More About This Article

Additional resources and features associated with this article are available within the HTML version:

- Supporting Information
- Access to high resolution figures
- Links to articles and content related to this article
- Copyright permission to reproduce figures and/or text from this article

View the Full Text HTML

ACS Publications
High quality. High impact.

Journal of the American Chemical Society is published by the American Chemical Society. 1155 Sixteenth Street N.W., Washington, DC 20036

J|A|C|S
ARTICLES

Published on Web 06/25/2008

Effect of Confinement in Carbon Nanotubes on the Activity of Fischer−Tropsch Iron Catalyst

Wei Chen, Zhongli Fan, Xiulian Pan,* and Xinhe Bao*

State Key Laboratory of Catalysis, Dalian Institute of Chemical Physics, Chinese Academy of Sciences, Zhongshan Road 457, Dalian 116023, P. R. China

Received February 1, 2008; E-mail: panxl@dicp.ac.cn; xhbao@dicp.ac.cn

Abstract: Following our previous findings that confinement within carbon nanotubes (CNTs) can modify the redox properties of encapsulated iron oxides, we demonstrate here how this can affect the catalytic reactivity of iron catalysts in Fischer−Tropsch synthesis (FTS). The investigation, using in situ XRD under conditions close to the reaction conditions, reveals that the distribution of iron carbide and oxide phases is modulated in the CNT-confined system. The iron species encapsulated inside CNTs prefer to exist in a more reduced state, tending to form more iron carbides under the reaction conditions, which have been recognized to be essential to obtain high FTS activity. The relative ratio of the integral XRD peaks of iron carbide (Fe_xC_y) to oxide (FeO) is about 4.7 for the encapsulated iron catalyst in comparison to 2.4 for the iron catalyst dispersed on the outer walls of CNTs under the same conditions. This causes a remarkable modification of the catalytic performance. The yield of C_{5+} hydrocarbons over the encapsulated iron catalyst is twice that over iron catalyst outside CNTs and more than 6 times that over activated-carbon-supported iron catalyst. The catalytic activity enhancement is attributed to the effect of confinement of the iron catalyst within the CNT channels. As demonstrated by temperature-programmed reduction in H_2 and in CO atmospheres, the reducibility of the iron species is significantly improved when they are confined. The ability to modify the redox properties via confinement in CNTs is expected to be of significance for many catalytic reactions, which are highly dependent on the redox state of the active components. Furthermore, diffusion and aggregation of the iron species through the reduction and reaction have been observed, but these are retarded inside CNTs due to the spatial restriction of the channels.

1. Introduction

Carbon nanotubes (CNTs) distinguish themselves from other carbon materials, e.g., activated carbon and carbon nanofibers, in that they have graphene layers with semiconducting or metallic characteristics and a tubular morphology.[1] Theoretical studies reveal that deviation of the graphene layers from planarity causes π-electron density to shift from the concave inner surface to the convex outer surface,[2–4] leading to an electron-deficient interior surface and an electron-enriched exterior surface. This should influence the structure and electronic properties of substances in contact with either surface. Menon et al. reported that the interaction of transition metal atoms with CNT walls differs significantly from their interaction with graphite layers with regard to bonding sites, magnetic moments, and charge-transfer directions.[5] This effect is envisioned to have potential for CNT applications in many fields such as magnetic materials, gas sensors, field emission and catalytic materials.[6,7]

We have previously found that the properties of Fe_2O_3 were modified significantly when the particles are encapsulated in CNTs. In particular, the autoreduction of Fe_2O_3 is facilitated within the CNT channels compared to that of those particles located on the CNT outer walls,[8] and the reduction temperature decreases monotonically with the inner diameter of CNTs.[9] A similar effect has been recently observed for Fe_3O_4 nanowires encapsulated inside CNTs.[10] This provides a novel way to modify the redox properties of the confined substances, and it is expected to be of significance for many catalytic reactions, which are highly dependent on the redox state of the active components.

Here we choose Fischer−Tropsch synthesis (FTS) over iron catalyst as a probe reaction to investigate how the confinement of the catalytically active components within CNTs would affect the catalytic performance. FTS is considered a promising route for converting natural gas, coal, and even biomass to liquid fuels and other chemicals via syngas. It is well known that the distribution of iron phases changes during reaction on-stream and the relative composition is closely related to the state of the iron catalyst.[11–14] Metallic iron is formed if the catalyst is reduced in H_2, which is readily converted to a mixture of metal,

(1) Ajayan, P. M. *Chem. Rev.* **1999**, *99*, 1787.
(2) Ugarte, D.; Chatelain, A.; de Heer, W. A. *Science* **1996**, *274*, 1897.
(3) Haddon, R. C. *Science* **1993**, *261*, 1545.
(4) Shan, B.; Cho, K. *Phys. Rev. B* **2006**, *73*, 081401.
(5) Menon, M.; Andriotis, A. N.; Froudakis, G. E. *Chem. Phys. Lett.* **2000**, *320*, 425.
(6) Baughman, R. H.; Zakhidov, A. A.; de Heer, W. A. *Science* **2002**, *297*, 787.
(7) Pan, X.; Fan, Z.; Chen, W.; Ding, Y.; Luo, H.; Bao, X. *Nat. Mater.* **2007**, *6*, 507.
(8) Chen, W.; Pan, X.; Willinger, M. G.; Su, D. S.; Bao, X. *J. Am. Chem. Soc.* **2006**, *128*, 3136.
(9) Chen, W.; Pan, X.; Bao, X. *J. Am. Chem. Soc.* **2007**, *129*, 7421.
(10) Cao, F.; Zhong, K.; Gao, A.; Chen, C.; Li, Q.; Chen, Q. *J. Phys. Chem. B* **2007**, *111*, 1724.

10.1021/ja8008192 CCC: $40.75 **© 2008 American Chemical Society**

carbides, and oxides under the reaction conditions. Among those phases, iron carbides are recognized to be essential to obtain high FTS activity.[11–13]

The use of CNTs as a support for FTS iron catalysts has been recently studied.[15–17] In those studies, iron was dispersed on the CNT outer walls, and the main focus was on the effect of additives such as copper and potassium and the catalyst preparation methods. In the present work, we intend to study the effects of confinement of catalyst within CNTs on the FTS activity and ultimately the feasibility of tuning the catalytic performance via changing the CNT dimensions. A patented method has been employed to introduce iron species into the channels of CNTs (Fe-*in*-CNT).[18] The FTS activity of Fe-*in*-CNT and product selectivities are compared to those of the catalyst with iron nanoparticles dispersed on the CNT outer walls (Fe-*out*-CNT) and on an activated carbon (Fe/AC). The contribution of the electron confinement and the spatial restriction within the CNT channels are discussed.

2. Experimental Section

2.1. Catalyst Preparation. The procedures have been reported previously for the preparation of the CNT-encapsulated iron oxide and iron oxide particles dispersed on the CNT outer walls.[9,18] Briefly, raw CNTs were first opened up and cut into segments of 200−500 nm long by refluxing in concentrated HNO_3 (68 wt %) at 140 °C for 14 h. The resulting CNTs have inner and outer diameters of 4−8 and 10−20 nm, respectively. Aqueous $Fe(NO_3)_3$ solution was introduced into the CNT channels utilizing the capillary forces of CNTs aided by ultrasonication and stirring. Subsequent drying and heat treatment at 350 °C in Ar resulted in CNT-encapsulated Fe_2O_3, denoted as Fe_2O_3-*in*-CNT. Before FTS, the catalyst was activated by reduction in a pure H_2 stream (100 mL/min) at 350 °C for 5 h (standard activation conditions unless otherwise stated). Thus, the activated Fe-*in*-CNT was obtained. The activated Fe-*out*-CNT catalyst was prepared by impregnating CNTs with closed caps in aqueous $Fe(NO_3)_3$ solution, followed by the same drying, heat-treatment, and reduction procedures. For comparison, we also dispersed iron particles on an activated carbon (Vulcan XC-72, Cabot Corp.), which had a BET surface area (237 m^2/g) similar to that of CNTs. The same procedure was followed to prepare the activated Fe/AC. The nominal loading of Fe in all catalysts was 10 wt %.

2.2. Catalyst Characterization. Transmission electron microscopy (TEM) was carried out on an FEI Tecnai F30 microscope and a G^2 microscope operated at an accelerating voltage of 300 and 120 kV, respectively. The samples were ultrasonically dispersed in ethanol and placed onto a carbon film supported on a copper grid.

The reducibility of Fe_2O_3-*in*-CNT and Fe_2O_3-*out*-CNT was studied by temperature-programmed reduction in H_2 (H_2-TPR) and CO atmospheres (CO-TPR). The process was monitored in situ by XRD on a Rigaku X-ray diffractometer equipped with an Anton-Paar XRK-900 reaction chamber. The sample was heated in flowing 10% H_2/Ar (H_2-TPR) or 10% CO/Ar (CO-TPR) up to 750 °C at a rate of 2 °C/min.

The crystal phase transformations of the iron catalysts during FTS were also studied by in situ XRD. The experiments were carried out under conditions close to those of the FTS reaction, i.e., syngas with H_2/CO volume ratio of 2, 270 °C, and 9.5 bar for 20 h. The pressure was limited due to the specifications of the reaction chamber. Diffraction patterns were recorded within a 2θ range of 30−50° because the most intense diffraction peaks of the relevant phases, i.e., Fe, FeO, Fe_2O_3, and iron carbides, fall in this range. The scanning rate was 10°/min. Patterns in a wider angle range (30−80°) were also taken from time to time at a scanning rate of 2°/min for the purpose of a more accurate identification of crystal phases.

2.3. Catalytic Reaction Tests. FTS was carried out in a stainless steel fixed-bed microreactor (7 mm inner diameter), in which 0.3 g of catalyst was packed. After the catalyst was activated by in situ reduction in pure H_2 at 350 °C for 5 h, the temperature was decreased to 270 °C in H_2. Syngas (H_2/CO volume ratio of 2) was then introduced at a flow rate of 100 mL/min, and the pressure was increased gradually up to a desired value (9.5−51 bar). The tail gas was analyzed online with a Varian CP-3800 gas chromatograph equipped with a Porapak Q column and a thermal conductivity detector. Liquid products were collected in a cold trap and analyzed off-line with a gas chromatograph equipped with an HP-5 capillary column. The CO conversion and product selectivities were determined only after the reaction had been running for at least 24 h under a given condition. Selectivity was reported as the percentage of CO converted into a certain product expressed in C atoms. C_2−C_4 refers to hydrocarbons containing 2−4 carbon atoms and C_{5+} to hydrocarbons containing 5 or more carbon atoms.

3. Results and Discussion

3.1. Reducibility of the Iron Catalysts. We studied the reducibility of iron oxide by H_2-TPR and CO-TPR monitored by in situ XRD. Figure 1 shows that Fe_2O_3 is converted first to FeO and then to metallic Fe in H_2 with increasing temperature, while Fe_2O_3 is transformed to FeO and then to metallic Fe and iron carbide (FeC and Fe_3C) in CO (Supporting Information, Figure S1). This stepwise reduction is in agreement with earlier studies.[19,20] The key temperatures of phase transformations are listed in Table 1 and compared with those reported earlier for the autoreduction process.[8,9]

It can be seen that the phase transformation of Fe_2O_3-*in*-CNT at each reduction step occurs at a much lower temperature than that of Fe_2O_3-*out*-CNT. For example, the reduction of Fe_2O_3 to FeO starts at 360 °C for the encapsulated iron catalyst, which is ∼100 °C lower than that for the outside catalyst during H_2-TPR. Metallic Fe appears 80 °C earlier in the encapsulated catalyst. During CO-TPR, Fe is detected at 420 °C, which is also 100 °C lower than in Fe_2O_3-*out*-CNT. In comparison, in the autoreduction process Fe_2O_3 is reduced to metallic iron in one step by CNTs, and the temperature difference is 200 °C between the inside and outside particles. This suggests that the iron oxide particles encapsulated within CNT channels are easier to reduce, regardless of the reducing agent. This is remarkable, considering that the diffusion of H_2 or CO in CNTs may slow the reaction to a certain extent with respect to the rate of reaction on the freely accessible CNT outer walls.

Although the particle size has been reported to affect the reduction,[21,22] TEM characterization shows that the iron oxide

(11) Raupp, G. B.; Delgass, W. N. *J. Catal.* **1979**, *58*, 348.
(12) Jung, H.; Thomson, W. J. *J. Catal.* **1992**, *134*, 654.
(13) Wang, P.; Kang, J. C.; Zhang, Q. H.; Wang, Y. *Catal. Lett.* **2007**, *114*, 178.
(14) Niemantsverdriet, J. W.; van der Kraan, A. M.; Delgass, W. N.; Vannice, M. A. *J. Phys. Chem.* **1985**, *89*, 67.
(15) Steen, E. V.; Prinsloo, F. F. *Catal. Today* **2002**, *71*, 327.
(16) Bahome, M. C.; Jewell, L. L.; Hildebrandt, D.; Glasser, D.; Coville, N. J. *Appl. Catal., A* **2005**, *287*, 60.
(17) Guczi, L.; Stefler, G.; Geszti, O.; Koppány, Zs.; Kónya, Z.; Molnár, É.; Urbán, M.; Kiricsi, I. *J. Catal.* **2006**, *244*, 24.
(18) Bao, X. H.; Chen, W.; Pan, X. L.; Fan, Z. L.; Ding, Y. J.; Luo, H. Y. Patent WO2007093081.
(19) Maiti, G. C.; Malessa, R.; Baerns, M. *Appl. Catal.* **1983**, *5*, 151.
(20) Yang, Y.; Xiang, H. W.; Tian, L.; Wang, H.; Zhang, C. H.; Tao, Z. C.; Xu, Y. Y.; Zhong, B.; Li, Y. W. *Appl. Catal., A* **2005**, *284*, 105.
(21) Kumar, D.; Varma, S.; Gupta, N. M. *Catal. Today* **2004**, *93*−*95*, 541.
(22) Kim, D. G.; Min, K. H.; Chang, S. Y.; Oh, S. T.; Lee, C. H.; Kim, Y. D. *Mater. Sci. Eng., A* **2005**, *399*, 326.

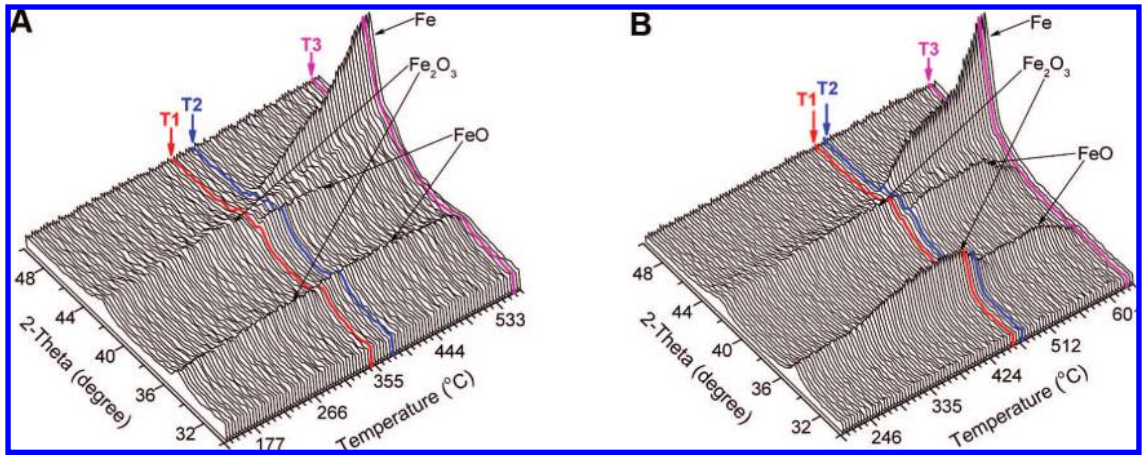

Figure 1. Temperature-programmed reduction in 10% H_2/Ar monitored in situ by XRD: (A) Fe_2O_3-*in*-CNT; (B) Fe_2O_3-*out*-CNT. T1, when FeO emerges; T2, when Fe appears; T3, when FeO disappears.

Table 1. Key Reduction Temperatures Detected by in Situ XRD during H_2-TPR, CO-TPR, and the Autoreduction Process

	T1 (FeO emergence, °C)			T2 (Fe emergence, °C)			T3 (FeO disappearance, °C)		
sample	H_2-TPR	CO-TPR	auto-red[a]	H_2-TPR	CO-TPR[b]	auto-red[a]	H_2-TPR	CO-TPR	auto-red[a]
Fe_2O_3-*in*-CNT	360	335	–	390	420	600	565	650	–
Fe_2O_3-*out*-CNT	455	450	–	470	515	800	620	735	–

[a] Reference 8. [b] At temperature T2, iron carbides form in parallel with Fe.

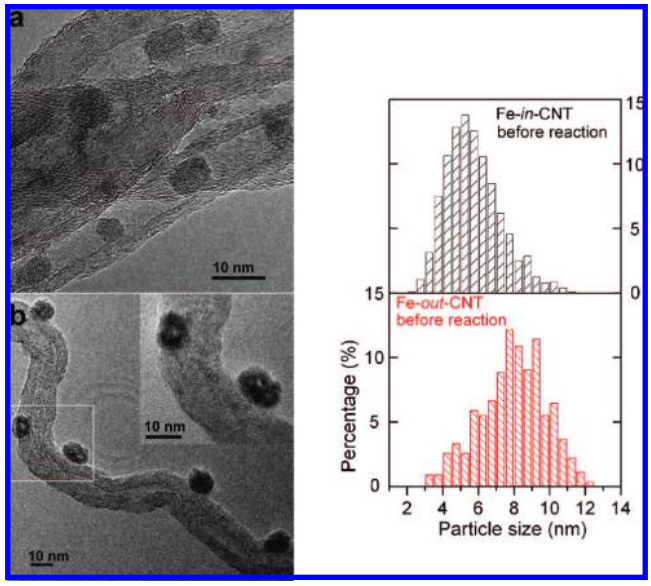

Figure 2. TEM images and particle size distribution of the activated catalysts (a) Fe-*in*-CNT and (b) Fe-*out*-CNT before reaction.

particles in the Fe_2O_3-*in*-CNT and Fe_2O_3-*out*-CNT catalysts are very similar in size, as we have observed previously.[9] Even after activation under rather strong conditions in pure H_2 at 350 °C for 5 h, the encapsulated Fe particles grow only slightly, and ~80% of the particles fall in the range of 4−8 nm (Figure 2 and Supporting Information, Figure S2). Those of Fe-*out*-CNT grow to 6−10 nm, which is not very significantly larger than the former. Therefore, we propose that the particle size difference is probably not a crucial cause of the notably modified reducibility of iron oxide observed in H_2-TPR and CO-TPR.

3.2. Phase Evolution of the Iron Species under FTS Reaction Conditions. After the in situ activation, the crystal phase evolution of the catalysts during FTS was studied by in situ XRD at 270 °C and 9.5 bar, which are close to the reaction conditions. The first curve, at 0 min time on-stream, in Figure 3A and the curve labeled "Fe-*in*-CNT before reaction" in Figure 3B show that the activated Fe-*in*-CNT exhibits strong diffraction of metallic Fe and weak diffraction of Fe_3O_4. Upon exposure of the catalyst to syngas at atmospheric pressure and 270 °C, metallic Fe rapidly decreases while iron carbides and oxide appear simultaneously. Formation of iron carbides and oxide is the result of the interaction of metallic iron with carbon and oxygen species from the dissociated carbon monoxide under the FTS conditions.[23,24] Although the most intense diffraction peaks of several iron carbides are very close to each other, the XRD pattern over a wider diffraction angle range (the curve labeled "Fe-*in*-CNT after reaction" in Figure 3B) shows that Fe_5C_2 and Fe_2C are the most likely carbides. We do not try to distinguish them further, and so we designate them Fe_xC_y. After FTS for 15 min, iron carbides increase to a stable intensity level and metallic Fe vanishes, indicating that Fe has been completely carburized. Fast carburization of Fe to Fe_5C_2 and Fe_2C has also been reported in earlier studies.[12] After 50 min on-stream, the syngas pressure is gradually raised from 1.0 to 9.5 bar, which increases the gas density in the reaction chamber, resulting in overall weakened diffraction peaks. After the pressure stabilizes, there is no further significant change in the iron oxide and carbides, implying that no further carburization occurs. The coexistence of Fe^{2+} and carbides has also been observed earlier during FTS under a H_2/CO ratio of 3.[14]

The changing trend of the main iron phases along reaction on-stream can be more clearly seen in Figure 3C. Note that the most intense peak of iron oxide overlaps with the peaks of CNT and Fe_3O_4 around 42.7°. Therefore, we demonstrate the phase changes by plotting the intensities of the 44.3° peak for metallic iron, 40.9° for carbide, and 36.9° for oxide, which do not overlap much with others. Figure S3 (Supporting Information) displays

(23) Niemantsverdriet, J. W.; van der Kraan, A. M.; van Dijk, W. L.; van der Baan, H. S. *J. Phys. Chem.* **1980**, *84*, 3363.
(24) Boudart, M.; McDonald, M. A. *J. Phys. Chem.* **1984**, *88*, 2185.

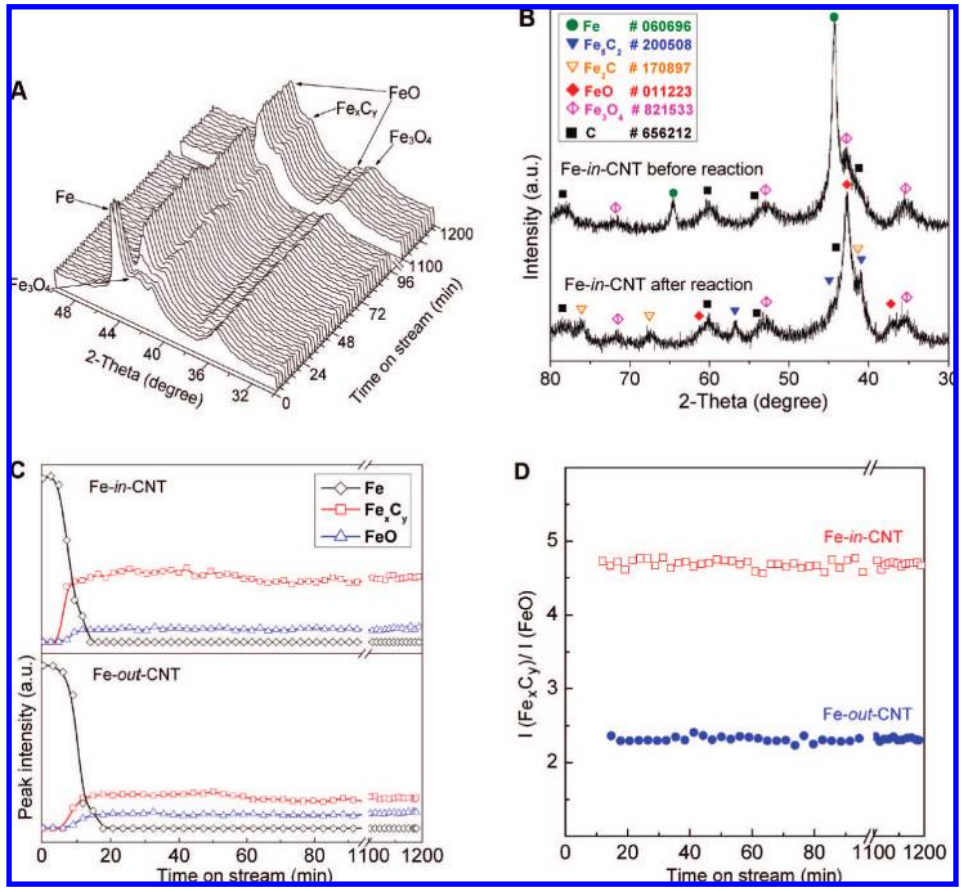

Figure 3. Crystal phase evolution of iron catalysts under conditions close to those of the FTS reaction (270 °C, syngas at 1.0−9.5 bar) during the time on-stream: (A) diffraction patterns of Fe-*in*-CNT; (B) diffraction pattern of Fe-*in*-CNT before and after FTS reaction for 20 h; (C) intensity of the diffraction peaks of metallic iron, iron carbide, and oxide; and (D) relative ratio of the integral peak areas of Fe_xC_y/FeO.

that Fe-*out*-CNT exhibits crystal phase transformations upon exposure to syngas similar to those observed for Fe-*in*-CNT.

For comparison of the relative concentration of iron carbides and oxides in these two catalysts, we estimate the relative ratio of the integral peak areas of iron carbide and oxide (Supporting Information, Figure S4). Figure 3D shows that the Fe_xC_y/FeO ratio is 4.7 for Fe-*in*-CNT after reaction for 15 min, and it does not change over 20 h. In contrast, this ratio in Fe-*out*-CNT is ∼2.4, much lower than that in the former catalyst. This implies that relatively more carbides have formed in the encapsulated iron catalyst during FTS. Catalysts with more carbide species were often found in earlier studies to exhibit higher FTS activity.[11,12,25–27] Therefore, we study the FTS activity over the Fe-*in*-CNT and Fe-*out*-CNT catalysts in the following section.

3.3. FTS Activity and Selectivity. Figure 4 shows the catalytic performance of the Fe-*in*-CNT and Fe-*out*-CNT catalysts during FTS as a function of the pressure. The reaction at low pressure does not yield much oil products due to the limited reaction rate, and the CO conversion is similar over both catalysts. With increasing pressure, the reaction is significantly accelerated, but much more so over Fe-*in*-CNT. At 51 bar, the CO conversion over Fe-*in*-CNT is ∼40%, which is 1.4 times that over Fe-*out*-CNT. The space−time yield of C_{5+} hydrocarbons is about 440 $g/kg_{cat}\cdot h$ over Fe-*in*-CNT, in comparison to 210 $g/kg_{cat}\cdot h$ over

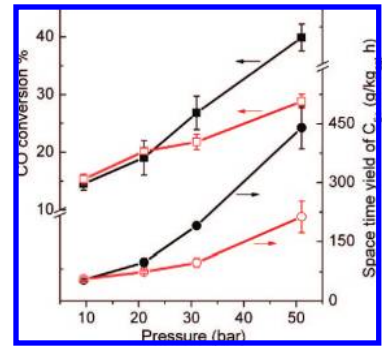

Figure 4. FTS activity of Fe-*in*-CNT and Fe-*out*-CNT at 270 °C as a function of pressure. Square symbols represent CO conversion and circles the space−time yield of C_{5+} hydrocarbons. Filled symbols denote Fe-*in*-CNT, while open ones denote Fe-*out*-CNT.

Fe-*out*-CNT. Note that blank FTS runs were carried out using CNTs without iron as catalyst, and almost no conversion was detected at 270 °C and 51 bar. This implies a negligible catalytic activity of blank CNTs for FTS. For comparison, we also dispersed the same loading of iron onto an activated carbon (XC-72), which has a BET surface area similar to that of CNTs, to obtain Fe/AC. As shown in Table 2 and Figure S5 (Supporting Information), the FTS activity of Fe/AC is much lower than that of both Fe-*in*-CNT and Fe-*out*-CNT over the whole pressure range.

Table 2 also shows that the selectivity of the shorter-chain hydrocarbons, including methane and C_2−C_4 hydrocarbons, is

(25) Dwyer, D. J.; Hardenbergh, J. H. *J. Catal.* **1984**, *87*, 66.
(26) Goodman, D. W.; Kelley, R. D.; Madey, T. E.; Yates, J. T., Jr. *J. Catal.* **1980**, *63*, 226.
(27) Dwyer, D. J.; Somorjai, G. A. *J. Catal.* **1978**, *52*, 291.

Table 2. Comparison of the FTS Activity and Product Selectivities at 51 bar

catalyst	CO conversion (%)	yield (g C_{5+}/kg_{cat}·h)	CO_2 selectivity (%)	hydrocarbon selectivities (%)		
				CH_4	C_2-C_4	C_{5+}
Fe-*in*-CNT	40	440	18	12	41	29
Fe-*out*-CNT	29	210	12	15	54	19
Fe/AC	17	61	5	15	71	9

lower and that of the longer-chain C_{5+} hydrocarbons is higher over the encapsulated iron catalyst than those over the outside catalyst. It is known that iron also catalyzes the water−gas shift (WGS) reaction during FTS, producing CO_2 and additional hydrogen. Therefore, the WGS activities over these two catalysts are compared by passing a stream of CO/Ar/He (10/5/85 vol %, 50 mL/min), saturated by water vapor at room temperature, to the catalyst bed, which is maintained at 270 °C. A CO conversion of 3.9% is obtained over Fe-*in*-CNT, in comparison to 1.6% over Fe-*out*-CNT, indicating a higher WGS activity over the encapsulated catalyst. Both CO_2 selectivities over these two catalysts fall in the range of 10−20%, in agreement with the value reported over a Cu-promoted Fe/CNTs catalyst.[15]

3.4. Effect of the Electron Confinement. The above results indicate that the reducibility of the CNT-encapsulated iron oxide has been significantly improved in both H_2 and CO. This is in accordance with our previous findings regarding the facilitated autoreduction of Fe_2O_3 encapsulated in CNTs compared to Fe_2O_3-*out*-CNT.[8] We proposed there that the electron deficiency of the interior CNT surface is possibly responsible,[8] because the π electron density of the graphene layers shifts from the inner to the outer surface of CNTs.[2−4] Thus, Fe_2O_3 should interact with the interior CNT wall differently from that with the exterior wall. This is reflected by the blue shift of the Fe−O vibration mode when Fe_2O_3 nanoparticles are moved from the outside to the inside of the CNT channels.[9] Within the channels, the electron density loss can be at least partially compensated through this interaction with the encapsulated Fe_2O_3, which can destabilize Fe_2O_3.[8,9] Our previous study on the CO adsorption on the bimetal Rh and Mn catalyst also implies that the state of Rh and Mn has probably been modified, leaving oxyphilic Mn in a more reduced state inside CNTs, which favors the adsorption of CO in a tilted form and hence the conversion of syngas.[7] The interaction of the encapsulated iron oxide with the interior CNT wall thus results in an easier reduction than occurs for the outside oxide. Although it is not clear to what extent the diffusion of H_2 or CO inside the CNT channels has impeded the reaction between Fe_2O_3 and H_2 or CO, the encapsulated Fe_2O_3 would have possibly exhibited even better reducibility than observed above. The result of the improved reducibility should favor the formation of more and stable reduced iron species in the activated Fe-*in*-CNT.

When this activated Fe-*in*-CNT is placed in the syngas atmosphere under FTS conditions, the interaction of metallic iron with dissociated CO results in a higher degree of carburizationdegree, as seen from the in situ XRD results. Similar effects of modification−improved reduction and hence carburization properties−are also observed when manganese is added to FTS iron catalyst as an additive, leading to a higher activity.[28] A monotonic correlation between the bulk carburization extent

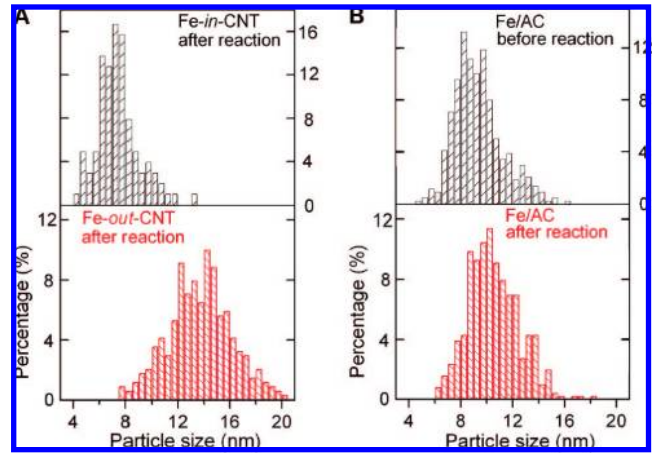

Figure 5. Particle size distribution of (A) Fe-*in*-CNT and Fe-*out*-CNT after reaction and (B) Fe/AC catalyst before and after reaction.

and the activity was frequently reported in earlier studies using XRD and Mössbauer spectroscopy.[11,12] Therefore, the higher CO conversion obtained over Fe-*in*-CNT can be at least partly attributed to its higher carbide content.

3.5. Effect of Particle Size. FTS on group VIII metals is known to be structure sensitive, and the particle size is one important parameter.[24] We find that the encapsulated iron particles remain similar in size to those prior to reaction, even after reaction for more than 200 h (Figure 5A and Supporting Information, Figure S6). Note that the Fe-*in*-CNT catalyst was further tested in reaction for 120 h at 51 bar and showed a very stable FTS activity, following the tests in Figure 4. For comparison, the size of the outside particles in Fe-*out*-CNT grew to ∼12−16 nm after the reaction tests in Figure 4. This indicates that particle sintering was effectively prevented inside CNTs under these reaction conditions due to the spatial restriction of the CNT channels.

There have been a few studies on the iron particle size effect on FTS,[17,24,29,30] which show that the specific activity decreases in general with decreasing crystallite size. For example, both methanation and C_2-C_5 production increase with the Fe particle size in the range of $1 < d/\text{nm} < 17.4$ around 250 °C.[24] Large iron particles or particle agglomerates have also been reported to be more active in formation of longer chains.[17] A similar particle size effect has been observed for cobalt.[31] A higher C_{5+} hydrocarbon selectivity is obtained over larger cobalt particles in a range of 2.6−15 nm, supported on carbon nanofibers.[31] However, recently Tang et al. reported a 2-fold increase in CO conversion over very small cobalt oxide particles (1.3−1.5 nm) inside the supercages of faujasite zeolites, compared to much larger particles (ca. 20 nm) on the outside of the supercages with a similar selectivity to C_{5+} hydrocarbons.[32] In comparison, the encapsulated iron (Fe-*in*-CNT) here also exhibits a 2-fold increase in the yield of C_{5+} hydrocarbons compared to Fe-*out*-CNT, although the particle size of the former catalyst (4−8 nm) is only slightly smaller than that of the latter (6−10 nm) after reduction. This reflects that particle

(28) Wang, C.; Wang, Q. X.; Sun, X. D.; Xu, L. Y. *Catal. Lett.* **2005**, *105*, 93.
(29) Jones, V. K.; Neubauer, L. R.; Bartholomew, C. H. *J. Phys. Chem.* **1986**, *90*, 4832.
(30) Jung, H. J.; Walker, P. L., Jr.; Vannice, A. *J. Catal.* **1982**, *75*, 416.
(31) Bezemer, G. L.; Bitter, J. H.; Kuipers, H. P. C. E.; Oosterbeek, H.; Holewijn, J. E.; Xu, X. D.; Kapteijn, F.; Dillen, A. J. D.; de Jong, K. P. *J. Am. Chem. Soc.* **2006**, *128*, 3956.
(32) Tang, Q. H.; Zhang, Q. H.; Wang, P.; Wang, Y.; Wan, H. L. *Chem. Mater.* **2004**, *16*, 1967.

size is not the only property to have an effect on the FTS activity. It is also worthy to note that Fe-*in*-CNT shows a very good FTS stability under a H_2/CO ratio of 2 at 270 °C, which contrasts with some earlier reports that the activity generally drops along reaction on-stream.[25,29]

For further clarification, we studied the morphology and particle size distribution of the Fe/AC catalyst before and after reaction. As shown in Figure S7 (Supporting Information), the particles are uniformly distributed. The particle size prior to reaction is ∼8−12 nm (Figure 5 B), which is larger than that of Fe-*out*-CNT before reaction. After reaction, the particle size of Fe/AC has increased only slightly but is smaller than that of the post-reaction Fe-*out*-CNT catalyst. However, the FTS activity is much poorer than that of Fe-*out*-CNT in the whole pressure range (Supporting Information, Figure S5). These results show that the particle size is not the only factor that leads to the significant difference in the catalytic performance of the Fe-*in*-CNT and Fe-*out*-CNT catalysts. The better reducibility due to confinement within CNTs may be more important for the improved FTS activity of Fe-*in*-CNT.

Furthermore, CNTs used in this study have an inner diameter of 4−8 nm and a length of ∼200−500 nm. Confinement of reaction intermediates within such nanochannels may prolong their contact time with the catalyst. This can favor the chain growth and lead to a higher selectivity to longer chain hydrocarbons inside CNTs.

4. Conclusions

The above results reveal that the confinement of iron inside CNTs does affect its catalytic performance. For example, FTS activity is notably increased when iron is confined within CNTs. The yield of C_{5+} hydrocarbons obtained over the encapsulated iron is twice that over the outside catalyst. TEM characterization of the catalysts and comparison to an iron catalyst supported on XC-72 activated carbon indicate that the iron particle size does not appear to be a crucial factor here for the significantly modified catalytic performance. We propose that the modified redox properties of the confined iron catalyst may play a more important role. H_2- and CO-TPR indicate that the reducibility of the encapsulated catalyst is remarkably improved in either H_2 or CO, although the diffusion of H_2 and CO into and out of the CNT channels may hinder the reduction process to some degree. This expedites the formation of more catalytically active carbide species during FTS. Furthermore, trapping of the reaction intermediates inside such channels likely prolongs their contact time with iron catalysts, favoring the growth of longer chain hydrocarbons. Thus, the encapsulated iron catalyst exhibits a higher FTS activity.

Acknowledgment. We thank Dr. Yingxia Wang from Beijing University for assistance in the XRD analysis and discussion. This work was supported by grants from the National Natural Science Foundation of China (Project Nos. 20503033 and 20573107) and the Ministry of Science and Technology of China (Project No. 2006CB932703).

Supporting Information Available: XRD patterns for CO-TPR, TEM images, and results of the FTS reaction of Fe/AC. This material is available free of charge via the Internet at http://pubs.acs.org.

JA8008192